Energy Deposition and Pressure wave dynamics in the International Linear Collider beam dumps

C. Densham, T. Davenne,* and O. Caretta
Rutherford-Appleton Laboratory, Didcot, Oxfordshire, OX11 0QX, UK

R. B. Appleby†
University of Manchester and the Cockcroft Institute, Oxford Road, Manchester, M13 9PL, UK

(Dated: August 18, 2008)

The International Linear Collider (ILC) requires four 18MW charged particle beam dumps, two for tune up purposes and two post-interaction point dumps. The baseline design is a scaled up version of a 2.2MW water beam dump which has been successfully employed at SLAC for many years. The motivation of this study was to investigate how pressure waves generated from the deposition of the ILC beam power compare with those generated in the SLAC dumps and whether this would pose significant technical issues. This paper describes simulations that have been carried out using Fluka and Autodyne to predict the response of the water contained within the dump following deposition of the ILC beam. Predictions of the induced pressures at the beam dump window and on the internal walls of the dump are presented for both the ILC and SLAC beams.

PACS numbers: 29.25.-t, 29.27.-a, 29.20.db

I. INTRODUCTION

The International Linear Collider (ILC) [1] is an international project to design and eventually build a TeV-scale electron positron collider. This machine is generally accepted to be the ideal partner machine for the Large Hadron Collider (LHC), and will aim for precision measurements of the particle content of the standard model and its extensions. The design of the ILC aims to collide bunches of electrons and positrons and study the resulting interactions. The virtue of the point-like collision particles is the precise knowledge of the collision energy. The machine parameters of the ILC aims for beam sizes at collision of a few nanometres in the vertical plane, with similar levels of beam stability. The particle energy at collision will be up to 500 GeV per beam, with a total collision luminosity of 1034 cm^{-2} s^{-1}. The accelerating cavities give a non-continuous time structure to the beams, with bunches of 2e 10 particle per collision and 2620 bunches arranged in a bunch train. The inter-bunch separation is of the order of 300ns, and the length of a train is around 1ms. The repetition rate of the design is 5 Hz, giving 5 bunch trains per second. The energy per particle, combined with the bunch size and time structure, gives a total maximum machine power of 17 MW per beam, with a corresponding time structure.

The ILC layout is comprised of a set of particle sources of electrons and positrons, which are accelerated to a particle energy of 5 GeV and damped to a small transverse size in a circular damping ring. The cooled beams are accelerated in a linear accelerator to the collision energy of between 250 GeV and 500 GeV, before being collimated and focused for collision in a beam delivery structure. The two beam collide at the interaction point (IP), and are then transported in an extraction line to a suitably designed beam dump. The purpose of the beam dump is to dispose of the post-collision particle beam and operate safely over the many-decade life of the machine. The performance rating of the beam dumps needs to be the maximum operating power of the machine, 17 MW, and must successfully dispose of this power with an AC time structure. Hence the requirements on the beam dump are very demanding. The baseline design consists of a single IP, with two identical accelerator machine. Hence the baseline requires two identical 17 MW beam dumps placed at the end of the corresponding extraction lines, and also two tune-up dumps at the end of each linear accelerator. In this work, only the disposal of the main charged beams are considered, and not the disposal of photons generated by the beam-beam collision or the dynamics of beam collimators and stoppers.

In section II the technology choices for the main beam dump, the baseline design of the dump system and the layout are described. The energy deposition into the water system, and the resulting formation of pressure waves, are considered in section III, and the dynamics of the window, both from direct beam interaction and from water system pressure waves, are the subject of sectionIV. Finally, the conclusions are presented in section V.

II. THE BEAM DUMPS

The technology choice for a beam dump is dependent on the particle energy and total power requiring disposal. All dump technologies consist of some form of absorptive media, which is placed in the path of the beam, coupled with an active cooling system if the absorbed power is high. The active cooling is generally necessary for all

*Electronic address: T.R.Davenne@rl.ac.uk
†Electronic address: robert.appleby@manchester.ac.uk

dumps beyond the simplest low power beam collimators, and most require some form of passive shielding. For low beam powers and particle energies, a solid-based dump is the good choice. This consists of sheets of a solid absorber, sandwiched between water cooling channels, and works for low to medium beam powers. For higher beam power, and the ILC, the solid dump cannot be cooled quickly enough and it becomes necessary to present the incident beam with a moving, and continuously recycling absorber. A water dump uses moving water, often in a rotating vortex, to absorb the incident power through an electromagnetic shower cascade which is then removed via a heat exchanger. This kind of dump was developed and used for the SLC [2], where it was built for a 2 MW beam and used successfully for many years. The ILC main beam dump is a scaling of the original SLC dump. Further technology choices can involve liquid metal beam dumps, or replacing the liquid with an absorbing column of noble gas [3]. This gas dump idea was developed for TESLA [ref] and the ILC, and remains a potential alternative for the ILC machine. The extraction line is the accelerator beamline which carries the beam from the interaction point to the beam dump window. The extraction line and the beam dump system are required to handle the highly spatially and angularly disrupted particle beam after a collision, aswell as the uncollided beam. The latter case gives a beam of smaller spatial extent and hence higher energy depositions in the beam dump system. The beam sizes on the dump window are calculated from beam transport simulations from the IP to the beam dump window, and consider the beam phase space characteristics and extraction line optical focusing elements. The results of these calculations provide the energy distribution into the window and water systems. The water-based beam dump for the ILC consists of 1.5m diameter cylindrical stainless steel high pressure water vessel. The water vessel is operated at 10 bar to raise the boiling temperature of the water. The heat is exchanged through a three-loop heat exchange system housed in the service cavern, with a capacity of 2300 gallons per minute. The dump is also equipped with a re-combiner to process the radiolytically produced hydrogen and oxygen, a storage tank for the dump water and a concrete-based radiation shielding system. The interface to the extraction line is provided by a 30 cm diameter 1 mm think Ti window, with a remote handling and replacement system. The incident beam on the beam dump window is swept in the extraction line by a pulsed magnet system designed to create a circular spot of radius 3 cm on the beam dump window during the passage of a 1 ms bunch train. The combination of the sweepers, the 10 bar pressure in the dump and the dump water vortex-flow circulation is designed to limit the temperature rise per bunch train to 40 Kelvin and prevent window damage from an undisrupted beam. The incident dump power is absorbed by 6.5 m of water (equivalent to 18 radiation lengths), followed by 1 m of water cooled Cu plates (22 radiation lengths).

III. ENERGY DEPOSITION INTO THE WATER SYSTEM

Fluka [4] has been used to determine the energy density deposited in water in units of GeV cm^{-2} per electron as a function of 3 dimensional space. A beam energy of 500GeV is assumed with 2620 bunches of electrons, each carrying 2e10 electrons being deposited in the water in 1ms. The energy deposited by a single bunch is 1.2kJ and by a complete bunch train is over 3MJ. The beam is rastored around a 30mm radius during that 1ms at a speed of 6.28e3 rads/s. This reduces the peak energy density in the water and the beam dump window. The beam window is eccentric to the axis of the 1.5m diameter cylindrical beam dump. Figure 1 shows an image of energy density contours in the cylindrical water beam dump after 0.54ms of a bunch train. Figure 2 shows the integrated energy deposited in the complete volume of water contained in the beam dump as a function of time. The interval between bunches is 300ns and the duration of a bunch is assumed to be 30ns. After a complete bunch train there is a 200ms gap before the next bunch train.

The energy deposition from each bunch of electrons causes an effectively instantaneous temperature rise in the water. This in turn results in a pressure rise which is proportional to the temperature rise [5]. Pressure waves will then move away from the region of increased pressure towards the walls of the beam dump. The first pressure wave has moved of the order 0.5mm before the next bunch of electrons is deposited in the water. The pressure waves of the successive bunches move towards the walls as more pressure pulses are added behind them. The pressure waves generated in the dump as a result of a bunch train of electrons have been modeled using Autodyne [6]. The peak pressure is observed at the axis of the beam and is found to be 13.5 bar above the design pressure of 10bar, as shown in figure 3. A complex map of pressure contours develops with some waves superposing upon each other and also a focusing of waves occurring at an eccentric axis opposite from the beam axis, figure 4. The maximum pressure experienced by the beam dump walls is predicted to be ∼8bar above the 10bar design pressure, figure 5, this results directly from the expansion of the high pressure region indicated in 4. The beam dump window region sees a maximum pressure rise of ∼4bar above the 10bar design pressure, as shown in figure 6. A summary of the internal pressures of interest as a function of time is given in figure 7.

By way of comparison with the SLAC water beam dump which has operated successfully for many years these simulations were repeated with the same characteristic dump dimensions but with the SLAC beam as the source of pressure waves. The SLAC beam energy was assumed to be 45GeV with 5.5x10^{11} electrons in each bunch making a total energy deposition of 5.4 kJ per bunch. After a bunch there is a 8ms gap before the next bunch. Figure 8 shows a summary of the predicted internal pressures with the SLAC beam and figure 9 compares the predicted window pressure with the SLAC and ILC beams.

The pressure waves produced by each bunch of electrons from both the ILC and SLAC beams are predicted to be elastic waves. The order of magnitude of pressure is not high enough for immediate formation of a shock wave by distortion of the Gaussian pressure wave that is formed as a result of the energy deposition. For SLAC which has a higher energy per bunch than ILC it was demonstrated that the induced pressure wave will not become a shock wave while it travels towards the wall of the dump [7]. Once at the wall of the dump the magnitude of pressure of each wave is significantly reduced due to radial spreading. Superposition of waves which occurs with the ILC dump where bunches are extracted in quick succession can give rise to some regions of high pressure after the bunch train has been extracted (see figure 4) however these pressures were never found to be higher than the peak pressure which was induced at the beam axis. No significant changes of density of the water were found during the Autodyne simulation also indicating that no shock waves are formed as a direct result of the energy deposition.

Aswell as elevated pressures above the design pressure of 10 bar some reductions in pressure below the design pressure were also observed. These occur at the axis of the beam as a result of cylindrical spreading of the pressure waves and also on reflection from internal surfaces of the beam dump. By virtue of the 10bar design pressure no negative pressures were observed at any point or location in the simulation. As such cavitation and the associated potential for damage to the internal surfaces of the beam dump due to micro jets and shock waves that form during the collapse of cavitation bubbles is not expected.

IV. DYNAMICS OF THE DUMP WINDOW

The beam dump window is one of the critical components in the design of the water beam dump. The baseline design for the window is a 15cm radius 1mm thick hemisphere made from Ti6Al4V. It is subjected to various stresses at various time scales, each of these is discussed in the following subsections.

A. Stress due to water pressure

The window has vacuum on one side and water at a design pressure of 10bar on the other side. In addition to this a pressure pulse of 4bar has been predicted to occur after each bunch train, i.e. at a frequency of 5Hz. The stress in the window has been calculated as a result of 14bar acting over the entire surface. As would be expected the peak compressive stress occurs at the rim of the window i.e. where the window is attached to the beam dump vessel. Figure 10 shows the stress contours when the rim of the window is constrained in a single direction only. If the rim of the window is constrained in all three directions then some tensile stress builds up around the rim (figure 11).

B. Stress immeadiately resulting from interaction of the beam with the window

Fluka has been used to calculate the energy deposition expected in the beam dump window. As the beam rastors around the surface of the window the energy deposition gives rise to a ring of material which is elevated in temperature by ∼7C. If we make the worst case assumption that this temperature rise is instantaneous then the stress is given by E$\alpha\Delta$T [5], where E is Youngs modulus (114GPa for Ti6Al4V), α is the thermal expansion coefficient (8.8x10-6 K^{-1} for Ti6Al4V) and ΔT is the temperature difference. This gives a stress wave magnitude of ∼7 MPa. An Autodyne model of the energy deposition in the window corroborates this value and also indicates that the stress waves traveling away from the point of energy deposition are negligible compared to the 7MPa induced by the beam. This is shown in figure 12. This is due to spreading of the waves causing the magnitude of stress to reduce significantly.

C. Stress due to time averaged differential thermal expansion

Heat will be conducted through the window away from the energy deposition area. Heat will also be transferred from the surface of the window to the passing water flow. A ring of material where the beam passes will be at an elevated temperature which depends on the conduction of heat through the window and the convection of heat from the surface of the window to the water. Consider a simple model of a slab of window material (figure 13). Assuming conduction through the window and convection to the water are the only two heat transfer processes the temperature difference between the point on the window where the energy is deposited and the water is given by

$$\Delta T = \frac{Q}{2kA}\sqrt{\frac{kA}{hP}}, \tag{1}$$

where k is the conductivity of the window material, 7.2W/mK, h is the convective heat transfer coefficient between the water and the window, a conservative figure of 500W/m2K has been assumed, Q is the heat flow in to the window material, 35W (calculated with Fluka simulation), A is the cross sectional area for conduction through the window, P is the perimeter of the conduction area and finally ΔT is the temperature difference between the temperature where the energy is deposited and the temperature of the water. The stress induced is proportional to the temperature difference i.e.

$$\sigma = E\alpha\Delta T. \quad (2)$$

ΔT is calculated as 35C and consequently the stress induced due to the differential thermal expansion is 35MPa.

The greatest stress on the window results from the water pressure and is cyclic in nature peaking at about 100 MPa. Stress caused by sudden heating of the window by the beam is of the order of 7 MPa and stress due to time averaged differential thermal expansion is no more than 35 MPa. The second two stresses occur in the region of the beam entry where as the stress due to water pressure occurs at the rim of the window. As such they are not superimposed and therefore the stress near the rim of the window due to the water pressure is the critical stress. The yield stress of Ti6Al4V is 1000 MPa, however the fatigue limit is between 100MPa and 600MPa [8] depending on pre-damage of a sample before cyclic testing. It therefore seems that the baseline window design is feasible but its success will be dependant on ensuring manufacture and installation without the introduction of imperfections which could trigger the reduced endurance limit.

V. CONCLUSIONS

The baseline design for the ILC main charged particle beam dump is a water beam dump based on the SLAC design. Transient pressures in the water beam dump have been predicted using a combination of Fluka and Autodyne. As a result of the higher power and different bunch structure of the ILC beam significantly larger transient pressures are predicted on the internal surfaces of the beam dump. The ILC beam dump window is expected to experience a 4 bar pulse compared to the predicted 0.04 bar for the SLAC window. This indicates that the successful experience with the SLAC beam dump window design may not be transferable to the ILC beam dump without consideration of this predicted cyclic pressure in the design.

The ILC beam dump window will be subjected to stress due to the water pressure, stress due to direct interaction with the beam and stress due to time averaged differential thermal expansion between the region where the beam impinges the window and the relatively cold rim of the window. The critical stress was found to be the compressive stress experienced at the rim of the window as a result of the water pressure. This is predicted to be 100MPa recurring at 5Hz (bunch train frequency). The endurance limit of the chosen titanium alloy is between 100 and 600 MPa indicating that the window must be manufactured and attached to the beam dump with careful consideration to avoiding any pre-damage of the window which could bring the material to the lower endurance limit.

[1] E. . Brau, J. et al. (ILC) (2007), 0712.1950.

[2] D. R. Walz, J. Jurow, and E. L. Garwin, EEE Transactions on Nuclear Science **NS-12** (1965).

[3] R. B. Appleby et al., The proceedings of EPAC06 (2006).

[4] A. A. Fasso, A. Ferrari, J. Ranft, , and P. R. Sala, CERN-2005-10, INFN/TC 05/11, SLAC-R-773 (2005).

[5] P. Sievers, *Elastic stress waves in matter due to rapid heating by an intense high energy particle beam* (1974).

[6] http://www.century-dynamics.com.

[7] T. Davenne, O. Caretta, and C. Densham, Submitted to Nuclear Instruments and Methods in Physics Research (2008).

[8] P. S. Prevey, N. Jayaraman, and R. Ravindranath, Proceedings International Conference on Fatigue Damage of Structural Materials V Hyannis, MA, Sept. 19-24 (2004).

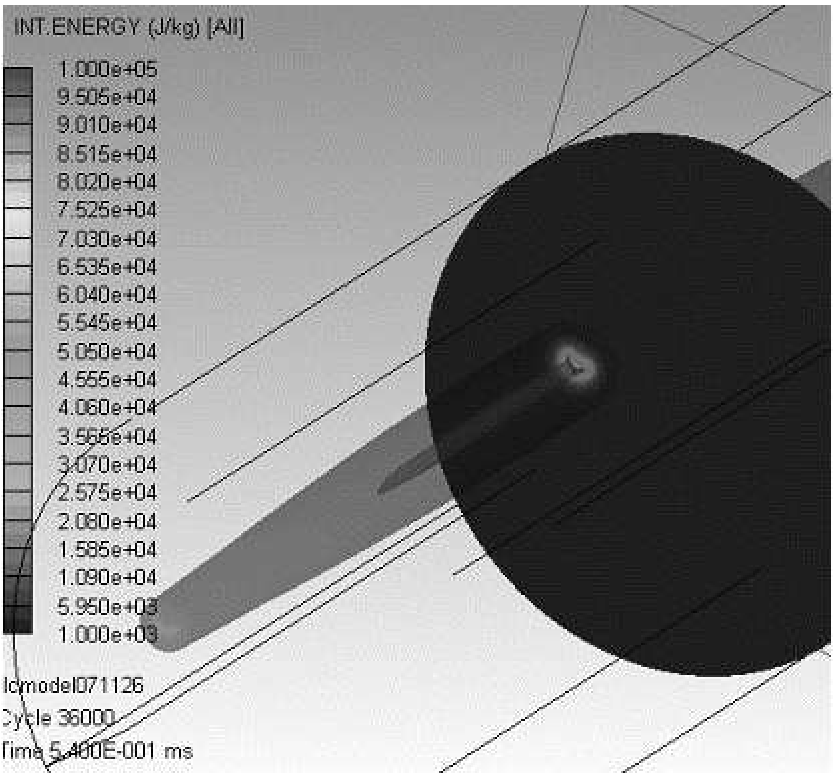

FIG. 1: The energy deposition of the particle beam into water.

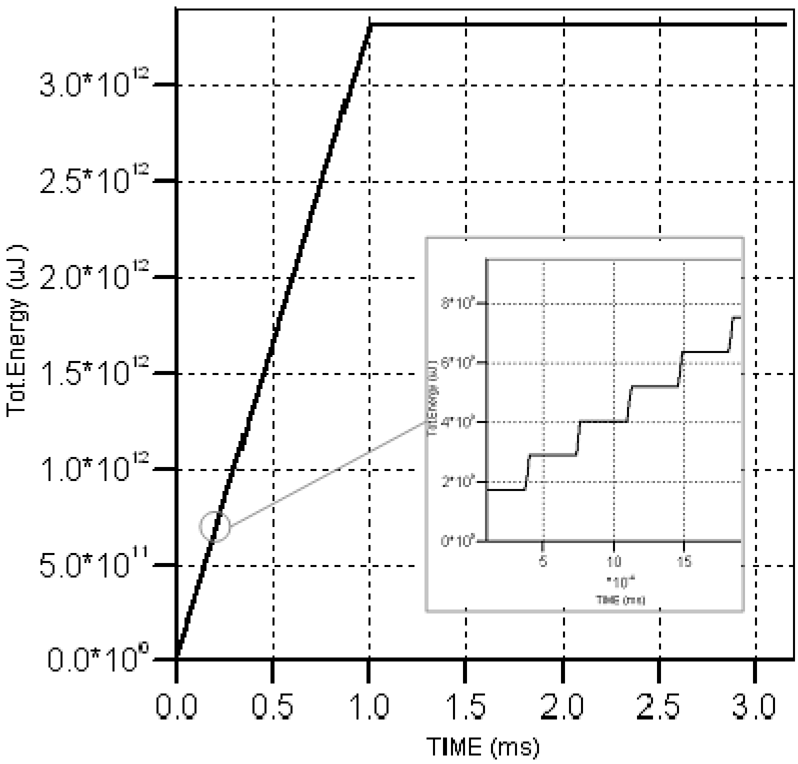

FIG. 2: Energy deposited in water beam dump in a single bunch train as a function of time.

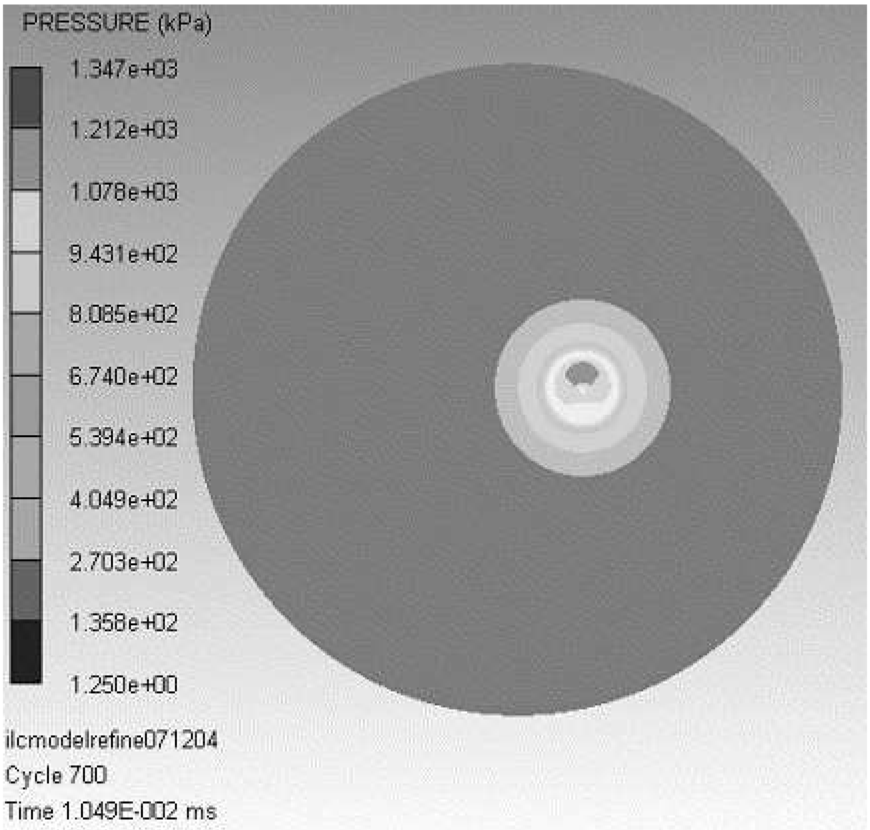

FIG. 3: Peak pressure at the axis of the beam.

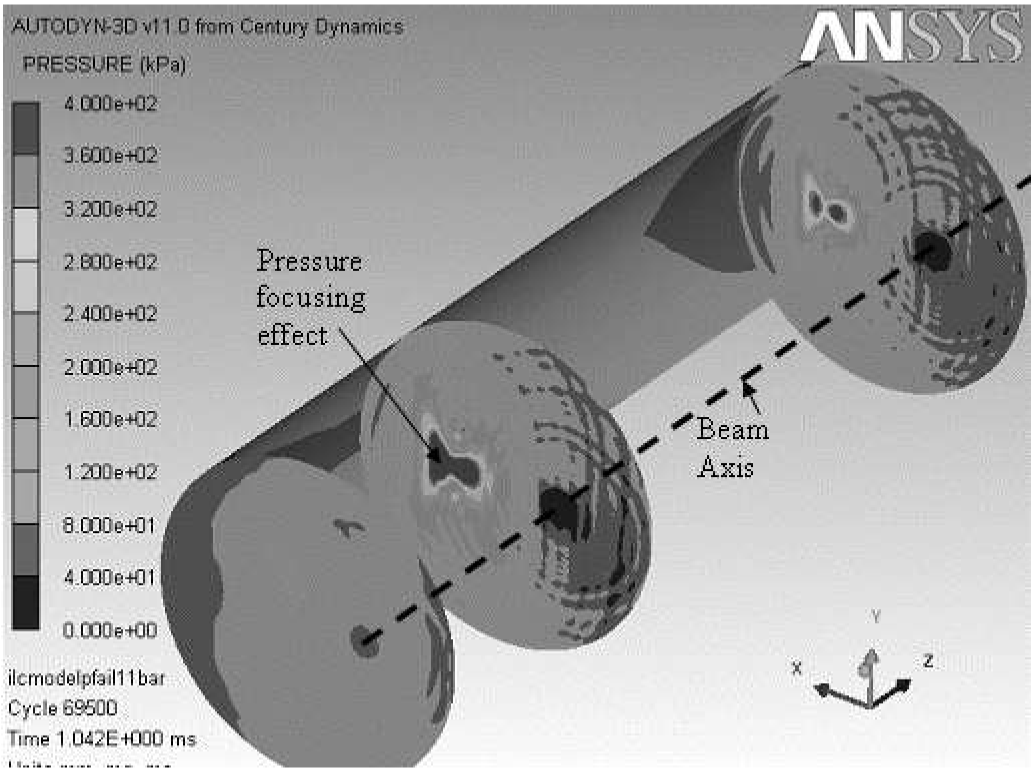

FIG. 4: Pressure contours after a complete bunch train.

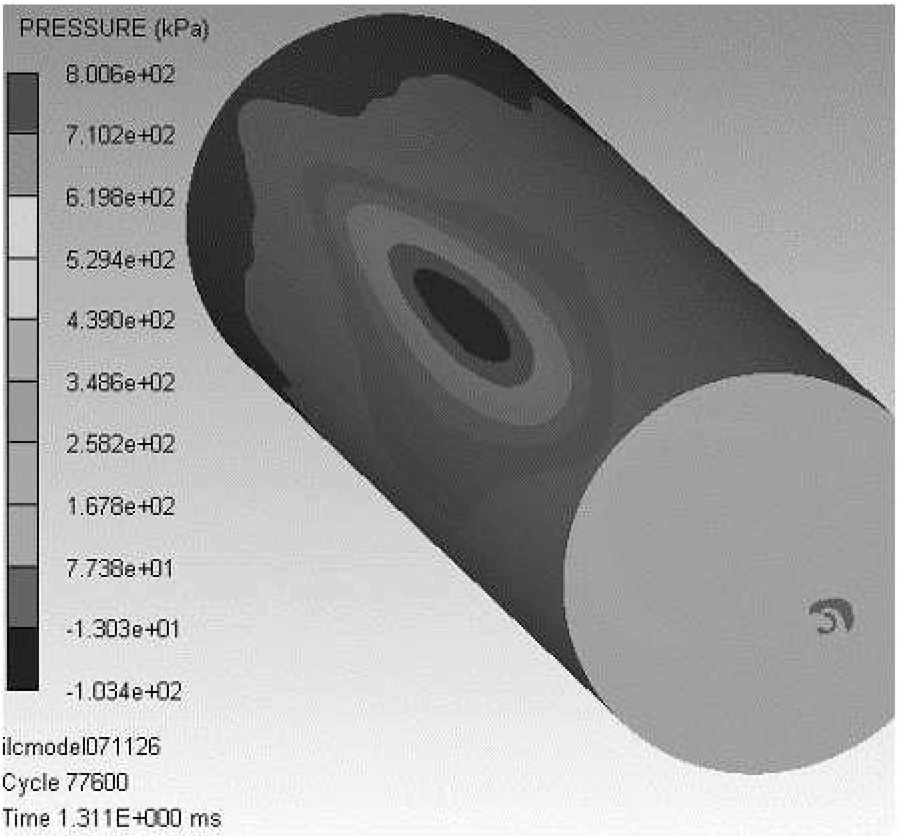

FIG. 5: Maximum pressure rise at the beam dump wall.

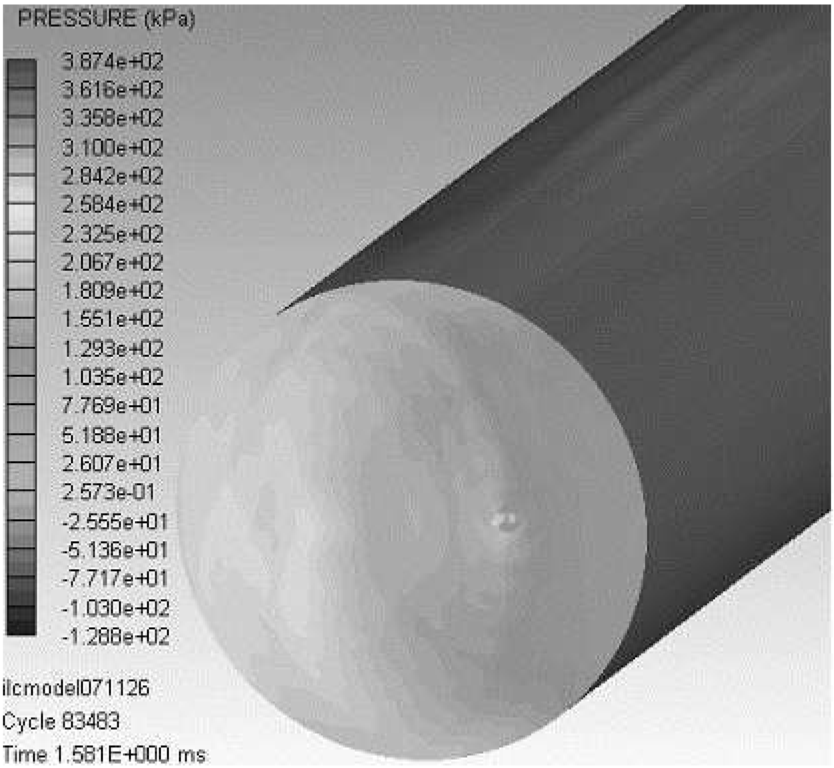

FIG. 6: Maximum pressure rise at the beam dump window.

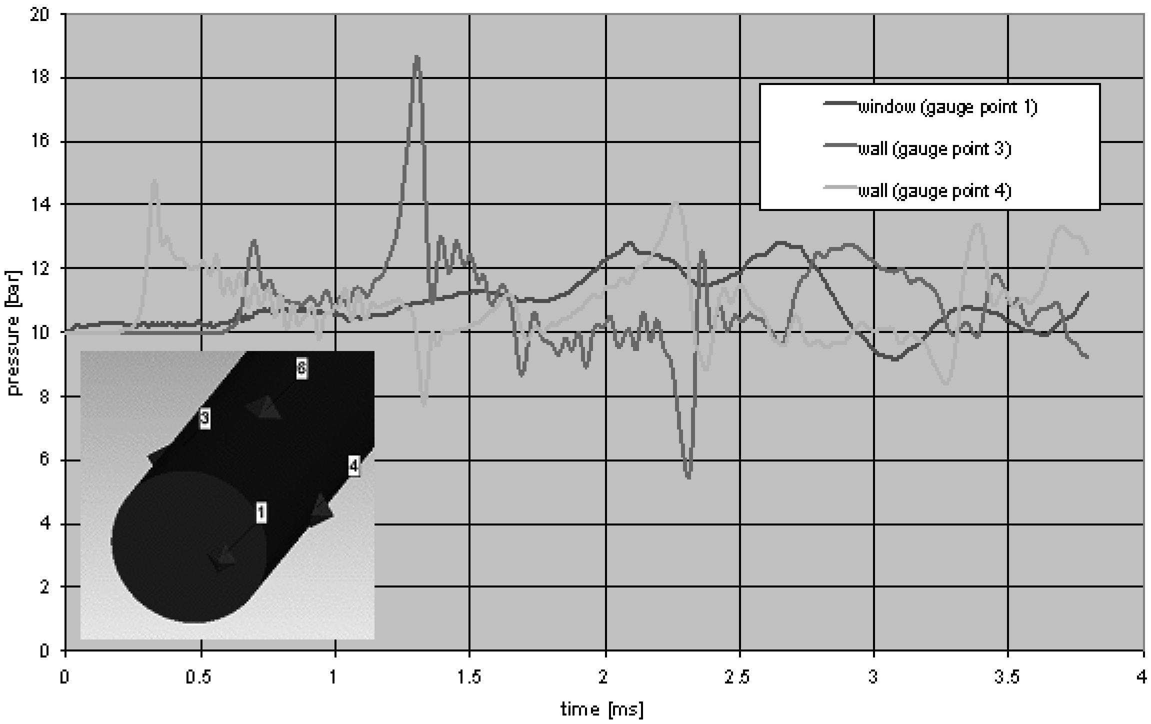

FIG. 7: Summary of beam dump internal pressures (ILC beam).

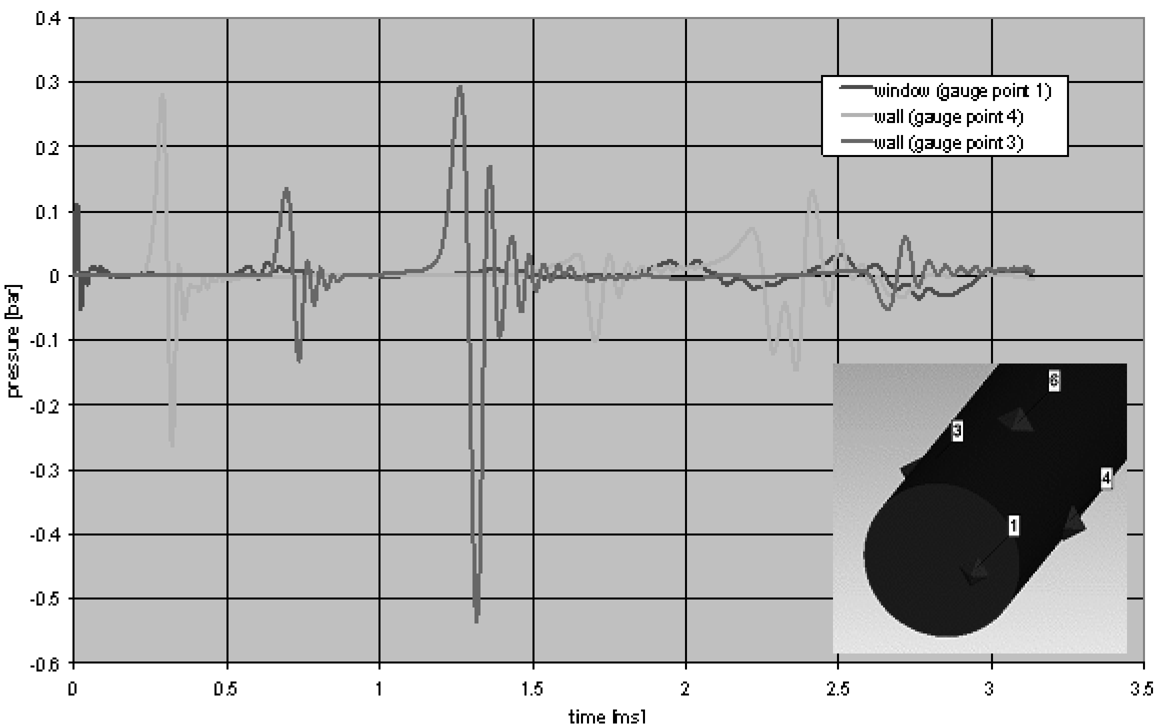

FIG. 8: Summary of beam dump internal pressures (SLAC beam).

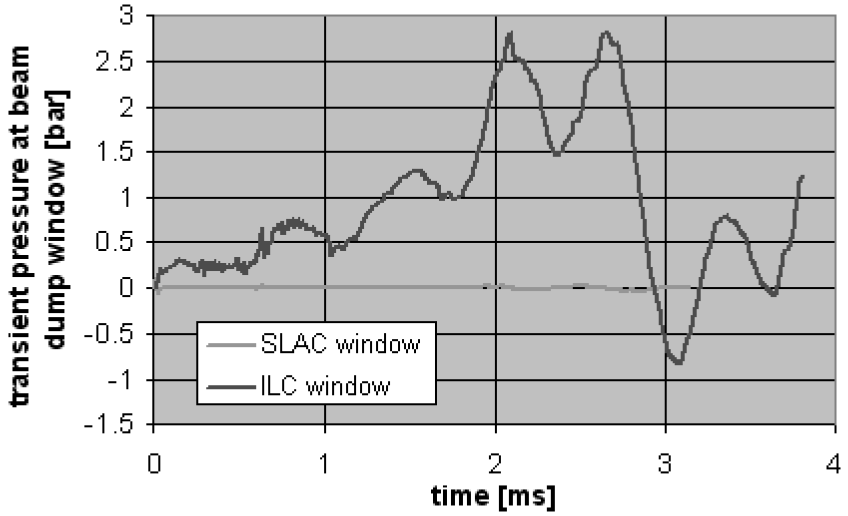

FIG. 9: Comparison of transient window pressure for ILC and SLAC.

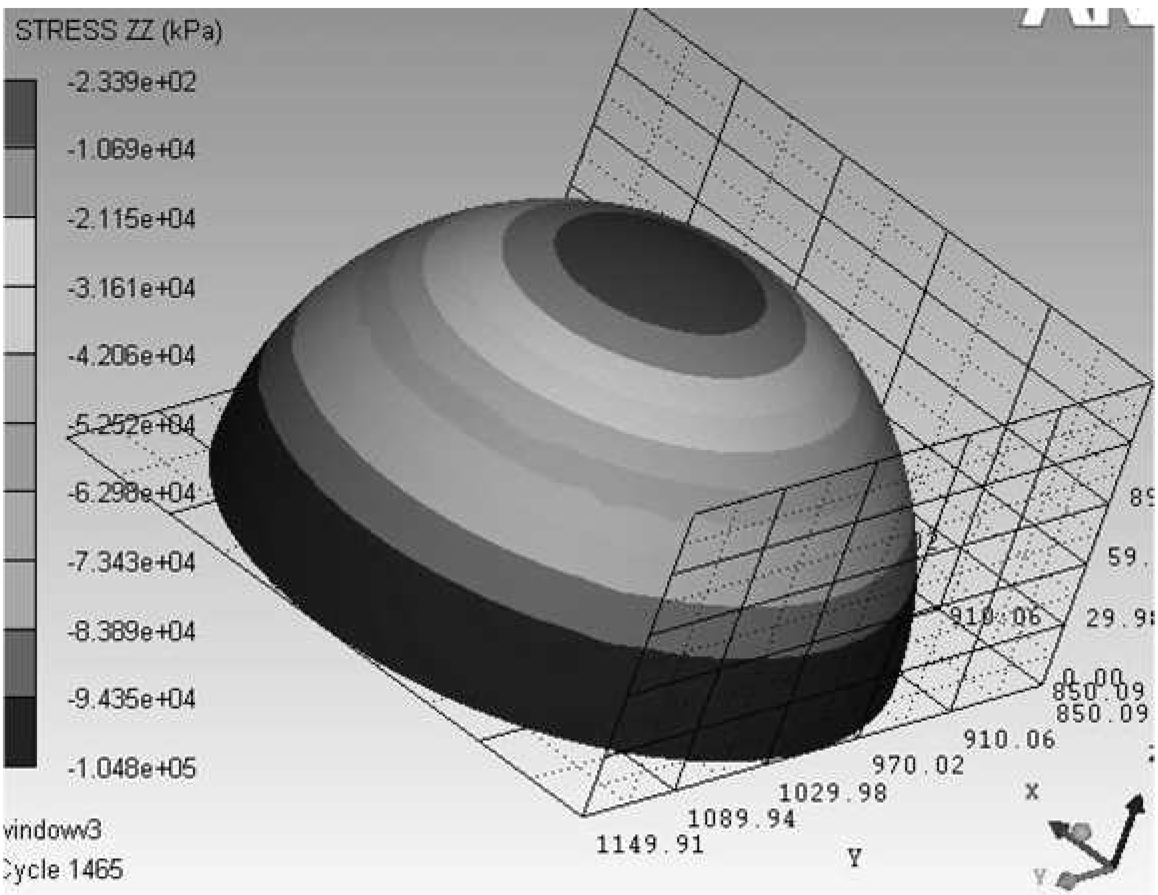

FIG. 10: Stress in hemispherical window due to water pressure of 14bar.

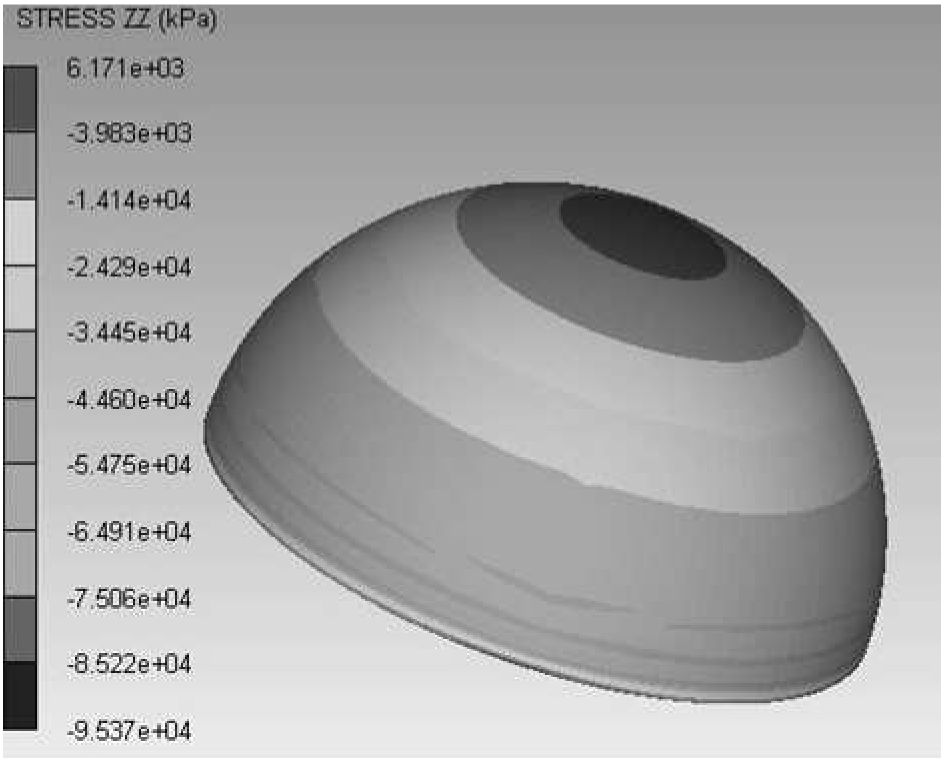

FIG. 11: The window constrained at rim in all three directions.

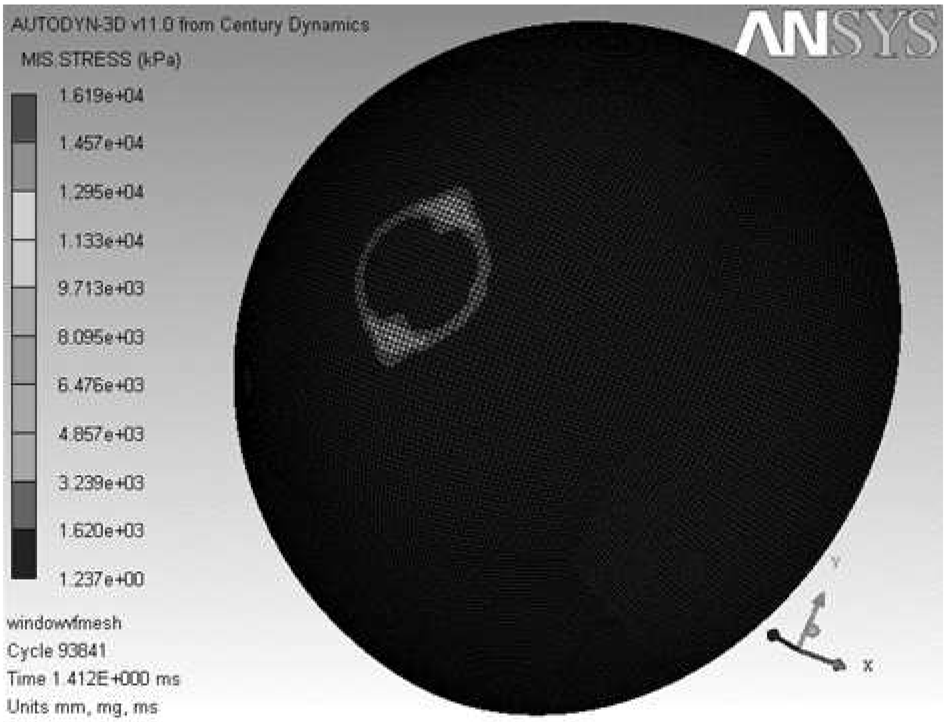

FIG. 12: Stress due to direct interaction of beam with the window.

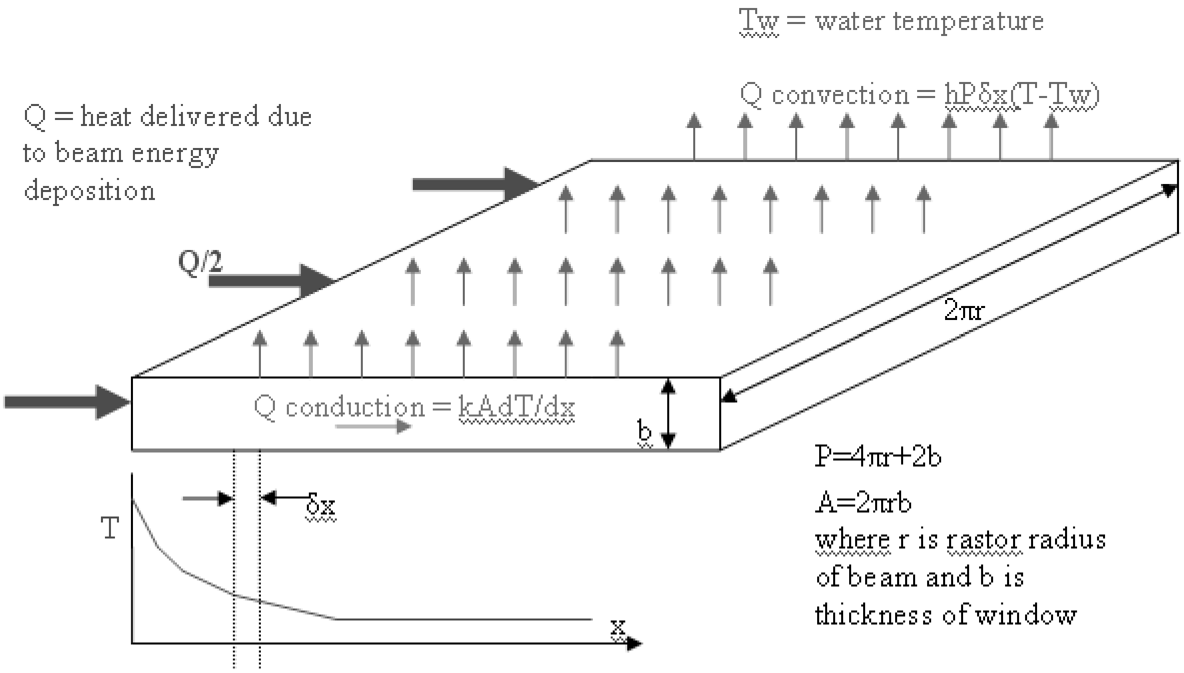

FIG. 13: The conduction and convection model.